atmosphere

MDPI

Article

Temporal Variation and Source Analysis of Atmospheric CH_4 at Different Altitudes in the Background Area of Yangtze River Delta

Meng Shan [1,2], Honghui Xu [2,*], Lujie Han [1,2], Yuting Pang [1,2], Juncheng Ma [1,2] and Chao Zhang [3]

1 Zhejiang Lin'an Atmospheric Background National Observation and Research Station, Hangzhou 311300, China; dfshanmeng@outlook.com (M.S.); xsxsxshh@gmail.com (L.H.); pangyuting816@163.com (Y.P.); agentzerov587@gmail.com (J.M.)
2 Zhejiang Institute of Meteorological Sciences, Hangzhou 310008, China
3 Quzhou Meteorological Bureau, Quzhou 324000, China; m13857039444@163.com
* Correspondence: forsnow@126.com

Abstract: Through an analysis of CH_4 data observed at different altitudes at the atmospheric background station in Lin'an from 2016 to 2020, in combination with back-trajectory and distribution characteristics of potential source areas, the CH_4 concentration variations at higher and lower altitudes and their relationships with sources and sinks were studied. The results showed that the CH_4 concentration was characterized by notable diurnal variations. The largest concentration difference occurred between 5 and 7 a.m.; the concentration difference in summer was higher than that in the other three seasons. Background filtering of the hourly CH_4 concentration was carried out using a numerical method. The results showed that the difference in the CH_4 background concentration between the two altitudes was 4.6 ppb (SD = 7.9). The CH_4 background concentrations at the two altitudes had the same seasonal variation: double peaks and valleys. The peaks appeared in May and December, and the valleys appeared in March and July. In spring and summer, the potential CH_4 source areas were mainly distributed in the rice planting and wetland discharge regions. In autumn, they were mainly distributed in regions affected by fugitive emissions from rice planting and coal mining. In winter, they were mainly distributed in livestock and poultry management regions.

Keywords: greenhouse gas; methane (CH_4); concentration characteristics; background concentration; source analysis

Citation: Shan, M.; Xu, H.; Han, L.; Pang, Y.; Ma, J.; Zhang, C. Temporal Variation and Source Analysis of Atmospheric CH_4 at Different Altitudes in the Background Area of Yangtze River Delta. *Atmosphere* **2022**, *13*, 1206. https://doi.org/10.3390/atmos13081206

Academic Editors: Junli Jin, Dongqing Fang and Mengyun Lou

Received: 9 July 2022
Accepted: 29 July 2022
Published: 31 July 2022

1. Introduction

Methane (CH_4) is an important greenhouse gas that causes global warming. Among anthropogenic greenhouse gases, its warming effect on the atmosphere is second only to that of CO_2. The 2020 Greenhouse Gas Bulletin issued by the World Meteorological Organization (WMO) showed that the average CH_4 concentration in 2020 was 1889 ± 2 ppb (parts per billion), that is, ~262% of that in 1750. Compared with the average CH_4 concentration in 2019, it increased by 0.59% (11 ppb). From 2018 to 2019, it increased by ~8.0 ppb [1]. The increase in 2020 is higher than the average increase in the past decade due to an increase in emissions from human activities. The CH_4 in the atmosphere mainly originates from emissions due to human activities, which account for ~60%, including fossil fuel and biomass burning, garbage landfills, rice cultivation, and ruminant emissions. Natural CH_4 release accounts for ~40% and includes wetlands, oceans, and termites [2]. CH_4 mainly reacts with OH radicals in the air, and the elimination reaction itself is the main sink of CH_4 [3,4]. CH_4 has a lifetime of ~10 years [5] and is one of the greenhouse gases controlled by the Tokyo Protocol.

In the 1970s, countries around the world began to observe atmospheric CH_4 concentrations, whereas China gradually started atmospheric CH_4 concentration observations in

the 1980s [6,7]. To further understand the concentrations and variations of atmospheric components in different regions of China, the China Meteorological Administration has successively deployed multiple atmospheric background stations to carry out long-term greenhouse gas observations.

In 1994, the China Meteorological Administration established an online observation system for greenhouse gases at the Waliguan Global Atmospheric Background Station in Qinghai Province. At the end of 2008, the China Meteorological Administration established CH_4 online observation systems based on cavity ring-down spectroscopy (CRDS) at four major atmospheric background stations (Waliguan Station in Qinghai Province, Lin'an Station in Zhejiang Province, Longfengshan Station in Heilongjiang Province, and Shangdianzi Station in Beijing City) [8]. The Yangtze River Delta region in China is relatively developed. Its rapid economic development has led to considerable greenhouse gas emissions. As the only atmospheric background station in East China, the Zhejiang Lin'an Atmospheric Background National Observation and Research Station (Lin'an Station, the same below) has received great attention.

At present, many scholars have discussed the CH_4 emissions based on different ecosystems and areas [9,10] and carried out studies on the CH_4 concentration based on urban sites [11,12]. Zhang et al. studied the CH_4 concentrations observed at atmospheric background stations in China and reported that the CH_4 concentrations are affected by regional emissions, and the variation characteristics of these sites were obviously different [13–16]. Cheng studied the variation of CH_4 along the coast of the South China Sea Pestunov and studied the CH_4 content in the atmosphere above Lake Baikal [17]. However, although observations of greenhouse gas at different altitudes have been carried out at many stations in China, there is a lack of studies comparing the background concentration of CH_4 at different altitudes. The influence of the near surface on the sources and sinks of CH4 can be analyzed, and variations in the characteristics of CH_4 at different altitudes can be obtained by studying its vertical profiles. Throughout the analysis of the variations in CH_4 concentration at different altitudes at Lin'an Station and the studies of the background concentration and sources, we will provide a basis for the formulation of greenhouse gas emission reduction policies in the Yangtze River Delta region.

2. Site Description and Methods

2.1. Site Description

Lin'an Station (30°18′ N, 119°45′ E, 138.6 m above sea level), which was established in 1983, is located in the west of Hangzhou City, Zhejiang Province, in the southwestern part of the Yangtze River Delta region, the largest economic zone in China. Lin'an Station is one of the first atmospheric background observation stations proposed by the WMO. It provides regional atmospheric composition background observations that are shared globally. The topography around the station mainly includes hills, woodlands, and farmland. The relative height of the hills is ~70 m. The woodland near the observation area mainly contains low pine forest and bamboo forest, and the vegetation coverage is good. There are no large villages within a radius of 3 km. The Lin'an station has four distinct seasons, the annual average temperature is 15.3 °C, and the annual average precipitation is ~1480 mm. The prevailing wind directions are mainly northeast and southwest. The occurrence frequency of special weather phenomena and inversion layers is very low, which is representative of the climate and atmospheric circulation characteristics of a typical subtropical monsoon region. The observation data can well represent the atmospheric background environment in the Yangtze River Delta region.

Lin'an station has been observing greenhouse gases for a long time. The station is equipped with a G2401 online observation system based on cavity ring-down spectroscopy (CRDS) developed by the Picarro Company in the United States. Greenhouse gases are observed at altitudes of 21 and 53 m. CH_4 observation sequences from 2016 to 2020 were selected for analysis.

2.2. Observation Data Quality Control

The sample gas was delivered to the greenhouse gas online observation system at Lin'an Station by two KNF vacuum pumps from the intake line, pulled down from 21 m and 53 m of the tower. After the sample gas was fully dried by the ultra-low temperature cold trap, its water vapor content was typically reduced to 0.001%, meeting the standard for stable measurements. Then, the sample gas was entered into the analysis module through an automatic injection control module. High and low altitudes were observed, and altitudes were switched every 5 min. The automatic injection control module can automatically select a 21 m air sample, 53 m air sample, working gas (W), and target gas (T) and inject it into the analysis system.

The original data were first manually filtered, and abnormal data, including those related to instrument failure and maintenance shutdown, were eliminated. The average value of 2 min after each 5 min data collection was selected for the analysis and processing.

2.3. Data Processing Method

The observation data included both background and non-background data. The background data from the region are mixed and uniform, and the non-background data are the data affected by local sources and sinks [18]. After manual quality control of the hourly average CH_4 data obtained at the two altitudes of 21 and 53 m in 5 years, the background, pollution, and low values of the two altitudes were obtained using a statistical approach called the robust extraction of background signal (REBS) and the IDP-Misc package of R software [19]. The width was set to 60 d, and the iterative calculation was carried out three times. There were 40,314 sets of valid CH_4 data at an altitude of 21 m, and after screening the data, 17,706 sets of these data (43.9%) could be viewed as background data. There were 41,919 sets of valid CH_4 data at an altitude of 53 m, and after screening the data, 18,445 sets of these data (44.0%) could be viewed as background data.

To study the effect of long-distance transmission of air masses in different seasons on the CH_4 concentration at the Lin'an Station, the HYSPLIT trajectory model was used for backward trajectory analysis, and the potential source contribution function (PSCF) was used to analyze the probability distribution characteristics of the potential source contribution.

The PSCF is defined as the conditional probability of a certain factor corresponding to the air mass reaching the observation point in the study area exceeding the set threshold. The study area was divided into several grids. The parameter N_{ij} is the total number of backward trajectories passing through the grid point (i, j), and M_{ij} is the number of high-concentration gas trajectories passing through the grid point (threshold concentration is the seasonal background average concentration after smooth fitting). The PSCF can be defined as:

$$PSCF_{ij} = M_{ij}/N_{ij}$$

To reduce the effect of the small number of total trajectories N_{ij}, the weight coefficient W_{ij} is set as follows:

$$WPSCF_{ij} = W_{ij} \times PSCF_{ij}$$

$$W_{ij} = \begin{cases} 1, N_{ij} > 60 \\ 0.7, 20 < N_{ij} \leq 60 \\ 0.42, 10 < N_{ij} \leq 20 \\ 0.05, N_{ij} \leq 1 \end{cases}$$

3. Results and Discussion

3.1. Diurnal Variation in CH_4 at Different Altitudes

Figure 1 shows the hourly average variation of the CH_4 concentration in different seasons (0:00–23:00, GMT+8). The diurnal variation trend of CH_4 at high and low altitudes is consistent; however, the diurnal variation characteristics in different seasons differ.

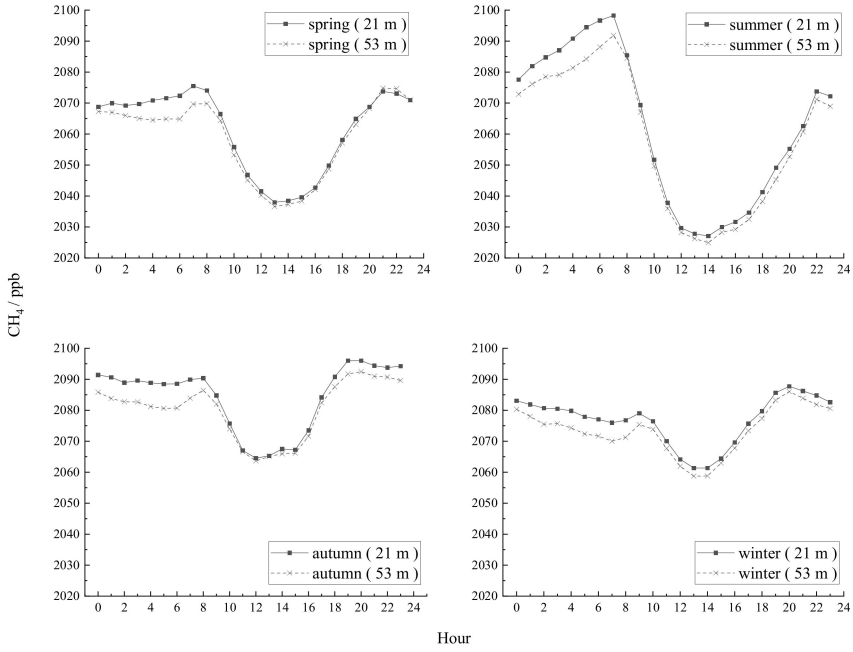

Figure 1. Hourly average CH_4 concentration changes at Lin'an Station.

In spring, the CH_4 concentration reaches its first low value at 0:00 and stabilizes at night. Due to the stable atmosphere at night, more CH_4 accumulates at lower altitudes, and the CH_4 concentration at lower altitudes increases slightly. The CH_4 concentration at higher altitudes decreases slightly and then increases. At ~8:00, the CH_4 concentration at both high and low altitudes reaches the first maximum and then rapidly decreases, reaching the minimum at ~13:00, because sufficient solar radiation during the daytime is conducive to the vertical movement of the atmosphere and creates more favorable diffusion conditions for CH_4. At the same time, direct solar radiation enhances the photochemical reaction between CH_4 and OH radicals, resulting in a stronger CH_4 sink during the daytime and a decrease in the CH_4 concentration. After 13:00, the CH_4 concentration rapidly increases and reaches the second maximum at ~21:00. In general, the CH_4 concentration at night is higher than that in the daytime, and the change in the CH_4 concentration at night is more stable. The difference between the two altitudes is larger between 0:00–8:00 than that during other periods because the boundary layer height is stable at night and the near-surface atmosphere is stable due to the decrease in the near-surface temperature, which is not conducive to CH_4 diffusion. In summer, the diurnal variation in the CH_4 concentration is the largest. At night, due to the stable atmosphere near the ground, the CH_4 concentration at the two altitudes gradually increases, reaching its maximum during the day at 7:00, and then rapidly decreases. The decline rate is faster than that in spring. This is due to the stronger solar radiation in summer, resulting in stronger CH_4 sinks and diffusion conditions. The CH_4 concentration eventually reaches a minimum at ~14:00. In autumn, the overall change in the CH_4 concentration is similar to that in spring. The minimum and maximum are reached at ~12:00 and ~20:00, respectively. In winter, the change range is the smallest. The minimum and maximum can be observed at ~14:00 and ~20:00, respectively.

Figure 2 shows the variation in hourly CH_4 concentration in different seasons (0:00–23:00, GMT+8). Overall, the variation in the CH_4 concentration difference at the two altitudes in different seasons is similar for each day. The CH_4 concentration at the lower altitude is higher than that at the higher altitude. The difference in the CH_4 concentration in the four seasons at the two altitudes reaches the maximum between 5:00–7:00. After sunrise, the difference in the CH_4 concentration at the two altitudes rapidly decreases and stabilizes in the afternoon. After a brief increase in the evening, it decreases for the second

time, especially in spring and summer. At night, the low temperature and weak vertical motion of the atmosphere are not conducive to CH_4 diffusion. The difference between the two altitudes gradually increases and reaches its maximum before sunrise.

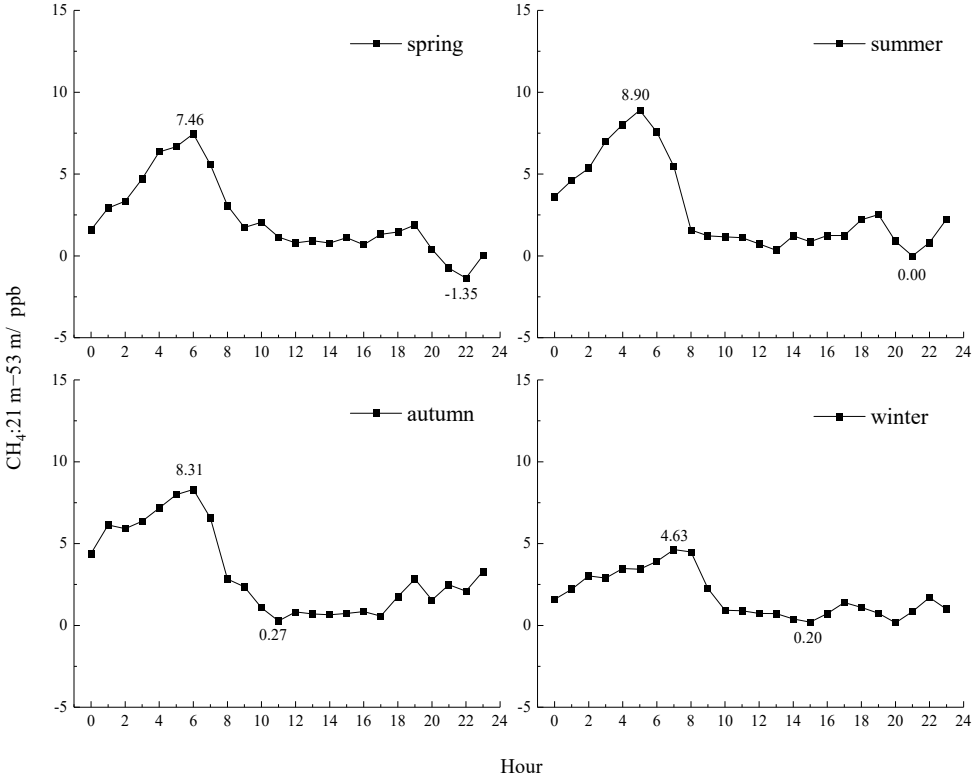

Figure 2. Difference in hourly CH_4 concentration in different seasons at the Lin'an station.

Figure 3 shows the temperature profile of the day in 2020, on which the extreme value of the CH_4 concentration difference between high and low altitudes was observed at 6:00 and 14:00 (0:00–23:00, GMT+8). The maximum value of the CH_4 concentration difference between the higher and lower altitudes (48.0 ppb) at 6:00 was observed on 31 July 2020. The minimum CH_4 concentration difference between the higher and lower altitudes (−19.6 ppb) at 6:00 was observed on 30 August 2020. The maximum CH_4 concentration difference between the higher and lower altitudes (23.8 ppb) at 14:00 was observed on 6 July 2020, and the minimum CH_4 concentration (−5.6 ppb) was observed on 31 August 2020.

On both 31 July 2020, and 30 August 2020, the two days when the extreme value of the CH_4 concentration difference between high and low altitudes appeared at 6:00, the inversion height was near the ground and the atmosphere was in a stable state. On both 30 August 2020, and 6 July 2020, the two days when the extreme value of the CH_4 concentration difference between high and low altitudes appeared at 14:00, due to the increase in the solar radiation, the near-surface temperature significantly decreased with the height and the atmosphere in an unstable state, which produced notable atmospheric convection and was conducive to CH_4 diffusion.

In general, the difference in the CH_4 concentration between high and low altitudes in winter is lower than that in the other three seasons. The difference in the CH_4 concentration between high and low altitudes in summer is higher than that in the other three seasons. In the Yangtze River Delta region, paddy fields and wetlands are the main sources of CH_4 emissions [20]. Paddy fields are the largest source of CH_4 emissions, and they only emit CH_4 during the rice-growing season, that is, from July to October. In winter, characterized by low temperatures, paddy fields do not emit CH_4. The CH_4 emission trend of wetlands is affected by temperature and precipitation [20]. In the Yangtze River Delta region, the amount of CH_4 emissions from wetlands generally reaches a peak between June and

August. The CH_4 concentration at Lin'an Station is greatly affected by local sources of emissions, which leads to a notable increase at lower altitudes, especially in spring, summer, and autumn, which are characterized by higher temperatures.

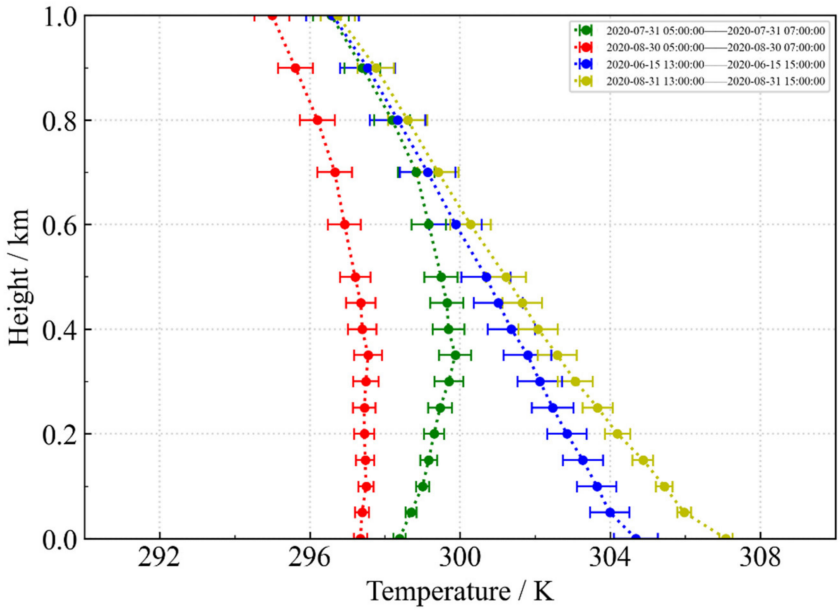

Figure 3. Temperature profile obtained at Lin'an Station on the day on which the extreme difference value was observed.

3.2. CH_4 Background Data Screening and Seasonal Variation

Table 1 shows the hourly CH_4 concentration at Lin'an Station from 2016 to 2020 after REBS screening. Figure 4 displays the hourly CH_4 concentration at Lin'an station after REBS screening, where BG represents the background value, POL represents the pollution value, and DEP represents the low value. The difference in the CH_4 background concentration between the two altitudes is 4.6 ppb, and the standard deviation is 7.9 ppb. In summer, the difference in the CH_4 background concentration between the two altitudes is the largest (9.7 ppb). In the other three seasons, the difference is smaller than the average value. Because the CH_4 concentration at Lin'an Station is greatly affected by local sources, the CH_4 concentration will increase significantly at a lower altitude, which is reflected in the screening results. The background value of the CH_4 concentration at the lower altitude is nearly double that at the higher altitude in summer, which indicates that the CH_4 data obtained at the higher altitude at Lin'an Station are more representative.

Table 1. Hourly CH_4 concentration at Lin'an Station from 2016 to 2020 after REBS screening.

Season	21 m CH_4 Concentration/ppb			53 m CH_4 Concentration/ppb		
	BG	POL	DEP	BG	POL	DEP
Spring	2028.3	2147.2	1974.0	2024.6	2144.7	1971.5
Summer	2002.2	2162.6	1924.4	1992.5	2157.0	1919.4
Autumn	2045.2	2172.0	1979.0	2040.2	2168.2	1975.1
Winter	2041.0	2163.3	1989.0	2037.8	2159.8	1986.3
Total	2031.0	2161.4	1963.2	2026.4	2157.5	1960.4

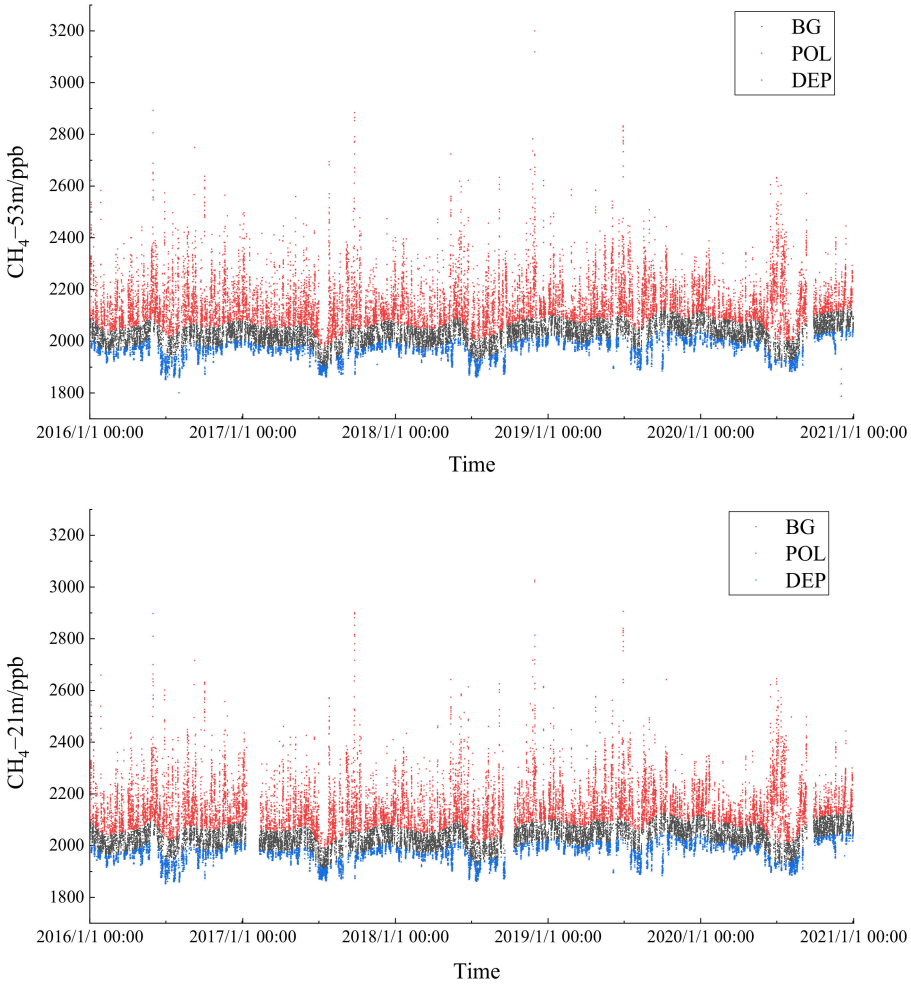

Figure 4. Hourly CH_4 concentration at Lin'an station after REBS screening.

Figure 5 shows the average monthly variation in the CH_4 concentration at two altitudes after REBS screening. The background concentration of CH_4 at high and low altitudes has the same temporal patterns, showing a double peak and double valley. The peaks appear in May and December, and the valleys appear in March and July. Specifically, the CH_4 background concentration is higher in winter. The CH_4 background concentration decreases from January to March and then gradually increases to the first peak in May. In summer, the OH concentration in the atmosphere is high due to the high concentration of O_3 near the surface in the Yangtze River Delta [21], and the CH_4 sink is more intense. Furthermore, there is more sunshine in summer, which is conducive to atmospheric diffusion. Therefore, the CH_4 background concentration reaches its minimum in summer and then gradually increases and reaches its maximum in December.

3.3. Cluster Analysis of Back Trajectories and Potential Source Analysis

To further study the effect of long-distance transport of polluted gas on the background concentration of CH_4 at Lin'an Station, a backward trajectory simulation was carried out using the trajectory analysis module of the MeteoInfo software, which was compiled by Wang et al. [22], and is based on GIS (Geographic Information System) data. The meteorological data used in this study are GDAS data from the global data assimilation system provided by the National Center for Environmental Prediction (NCEP). The starting times of the backward trajectory were 0:00, 6:00, 12:00, and 18:00 (0:00–23:00, GMT+8), and the height of the starting point of the backward trajectory was set to 500 m. Considering

the lifetime of CH_4 in the atmosphere, the backward time was set to 120 h. All trajectories were clustered based on the seasons (spring: March–May, summer: June–August, autumn: September–November, and winter: December–February). Based on the screening results, the average CH_4 background concentration in each season was used as the boundary between the background and pollution concentrations. After excluding the minimum, statistical cluster analysis results were obtained. Based on the above-mentioned analysis, the CH_4 concentration at higher altitudes better represents the background of the region. Therefore, these data were used for the cluster and potential source analyses. The potential source model (PSCF) was used to identify the distribution of areas with potential CH_4 emissions at Lin'an Station in different seasons (Figure 6). The deeper the color, the higher the probability of a potential CH_4 emission source area in this region.

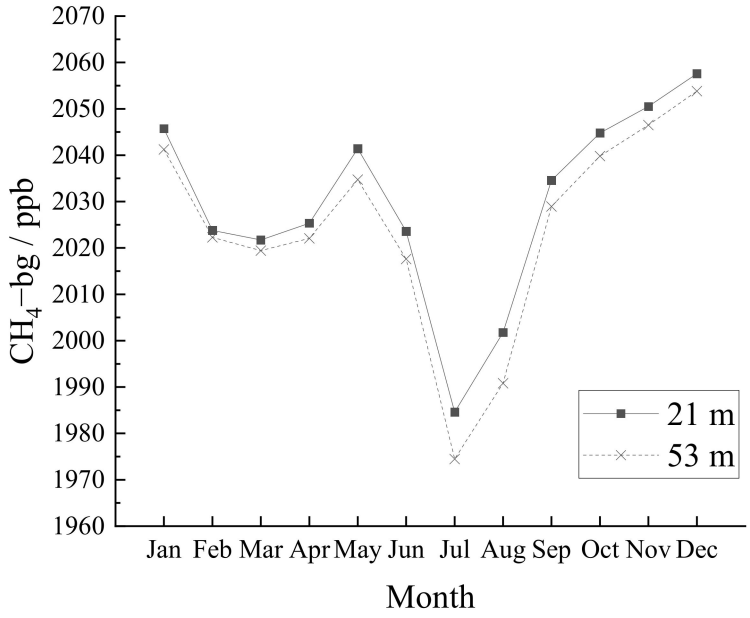

Figure 5. Seasonal variations in the CH_4 background concentration at Lin'an station.

In spring, the dividing point of the CH_4 background concentration and pollution concentration was 2024.6 ppb. The trajectory clustering characteristics are shown in Figure 7. Cluster 1 corresponds to the trajectory from Guizhou Province to Hunan Province and Jiangxi Province, and the number of trajectories accounts for $\frac{1}{4}$ of the total. The corresponding CH_4 concentration of cluster 1 is the highest, and the trajectory speed is slow. There are many provinces in the pathway, and the ground pollution in the pathway greatly affects the CH_4 concentration, which is significantly increased. Clusters 2 and 3 have a relatively high velocity, and the CH_4 concentration is relatively low. The proportion of cluster 4 is the largest, which corresponds to the trajectories passing through the sea route in Shanghai City and northern Zhejiang Province. The increase in the CH_4 concentration here is only second to cluster 1, indicating that the CH_4 concentration is greatly affected by human activities in the region. Potential source areas are mainly distributed in Shanghai City, eastern Zhejiang Province, northern Zhejiang Province, Nanchang City of Jiangxi Province, and northern Hunan Province. The CH_4 emission sources in these areas are similar and coincide with clusters 1 and 4. The main emission source is the paddy field. Early rice cultivation started in spring, which is an important factor affecting the background CH_4 concentration at Lin'an Station.

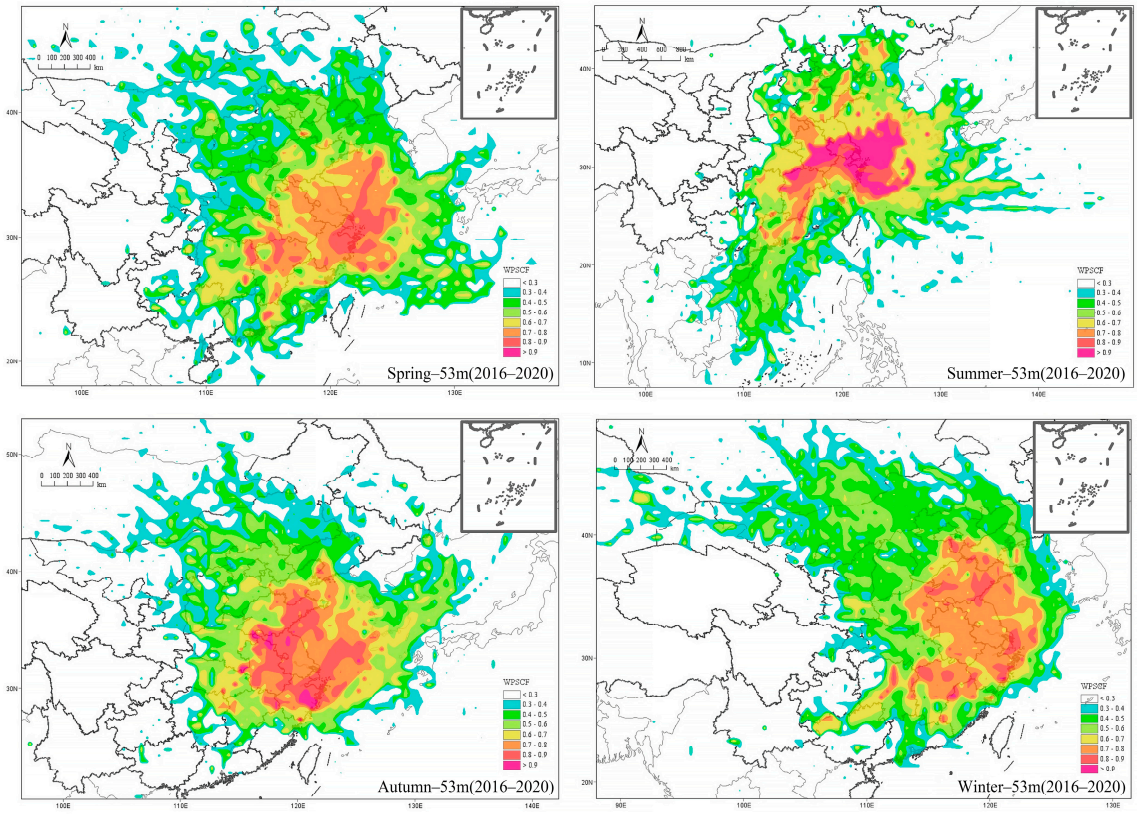

Figure 6. Potential CH_4 emission areas.

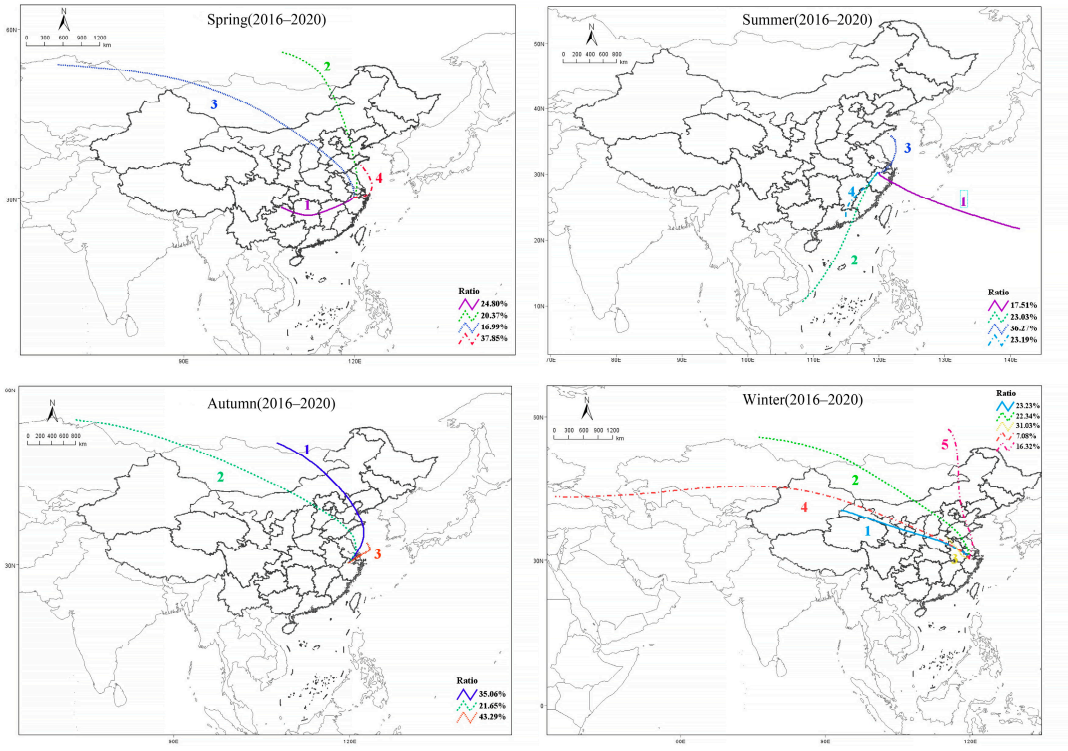

Figure 7. Trajectory clustering characteristics.

In summer, the dividing point between the CH_4 background concentration and pollution concentration is 1992.5 ppb. The trajectory clustering characteristics are shown

in Figure 6. Clusters 1 and 2 originate from the ocean, and the increase in the CH_4 concentration is relatively small. Cluster 3 has the largest number and a slow speed, which corresponds to the sea route trajectory in Shanghai City and northern Zhejiang Province. The corresponding CH_4 concentration is the highest, indicating that human activities in the region have a greater impact. Cluster 4 accounts for 1/4, which corresponds to the trajectory from Guangdong, passing through the provincial boundaries of Jiangxi Province, Fujian Province, and the western part of Zhejiang Province. The speed is slow, and the increase in the CH_4 concentration is second only to cluster 3. Potential source areas are mainly distributed in southern Jiangsu Province, northern Zhejiang Province, Shanghai City, southern Anhui Province, and northern Jiangxi Province. They coincide with clusters 3 and 4. These areas have dense water networks and numerous wetlands. Large-scale natural wetlands and paddy fields are important factors affecting the background CH_4 concentration at Lin'an Station.

In autumn, the dividing point between the CH_4 background concentration and pollution concentration is 2040.2 ppb. Trajectory clustering characteristics are shown in Figure 6. Cluster 3 originates from the ocean and passes through Shanghai City, southern Jiangsu Province, and northern Zhejiang Province with the slowest speed, largest number, and highest corresponding CH_4 concentration. In contrast, clusters 1 and 2 insignificantly increase the CH_4 concentration; cluster 1 has a relatively high CH_4 concentration due to its slow speed. Potential source areas are mainly distributed in Shanghai City, northern Zhejiang Province, and at the provincial boundaries of Anhui Province and Jiangsu Province. The areas with the deepest colors are Hangzhou City and the Shaoxing–Taizhou area of Zhejiang Province and Xuzhou City of Jiangsu Province. In the Yangtze River Delta region, the CH_4 emissions from paddy fields and coal mining account for 72.8% of the total anthropogenic emissions, whereas coal mining in the Yangtze River Delta region is mainly concentrated in Anhui Province and Xuzhou City of Jiangsu Province [23]. The emissions from coal mining in these regions also contribute to the increase in the CH_4 concentration at Lin'an Station.

In winter, the dividing point between the CH_4 background concentration and the pollution concentration is 2037.8 ppb. The trajectory clustering characteristics are shown in Figure 6. Cluster 3 has the largest number. It originates in Henan Province and arrives in Zhejiang Province through Anhui Province. The trajectory speed is the slowest, and the corresponding CH_4 concentration is the highest, which is greatly affected by ground pollution. Cluster 1 travels through multiple provinces from Xinjiang Province to Zhejiang Province, and the effect on the CH_4 concentration is relatively large. Potential source areas are mainly distributed in the Shaoxing–Taizhou area of Zhejiang Province, Nanchang City of Jiangxi Province, Changsha City of Hunan Province, and Shandong Province. In Jiangxi Province, Hunan Province, Shandong Province, and other regions, livestock is an important emission source in the winter [20] and an important factor affecting the background CH_4 concentration at Lin'an Station.

4. Conclusions

Based on an analysis of the CH_4 data observed at different altitudes at Lin'an Atmospheric Background Station from 2016 to 2020, the following conclusions can be drawn:

(1) The CH_4 concentrations at the high and low altitudes at Lin'an Station show notable diurnal variations, being high in the morning and evening and low in the daytime. The CH_4 concentration at the low altitude is higher than that at the high altitude. The diurnal variation of the CH_4 concentration difference at high and low altitudes is similar; in summer, it is higher than that in the other three seasons. The CH_4 concentration at Lin'an Station is greatly affected by local sources, which will lead to a significant rise in the CH_4 concentration at lower altitudes, especially in spring, summer, and autumn.

(2) The background CH_4 concentration at the higher and lower altitudes at Lin'an Station are 2026.4 and 2031.0 ppb, respectively, representing a difference of 4.6 ppb. The CH_4

concentration at higher altitudes is more representative of the region. The background CH_4 concentration at the two altitudes shows the same seasonal variation, that is, a bimodal and valley variation. Peak values can be observed in May and December, and minima appear in March and July.

(3) The potential source areas of CH_4 at Lin'an Station differ in different seasons. In spring and summer, the potential source areas are mainly distributed in the Yangtze River Delta region, Anhui Province, Jiangxi Province, Hunan Province, and other places that are greatly affected by rice planting and wetland discharge. In autumn, the potential source areas are mainly distributed in the Yangtze River Delta region and at the provincial boundaries of Anhui Province and Jiangsu Province, which are greatly affected by paddy fields and coal mining. In winter, the potential source areas are mainly distributed in the Shaoxing–Taizhou area, Nanchang City of Jiangxi Province, Changsha City of Hunan Province, and Shandong Province, which are greatly affected by livestock emissions.

Author Contributions: Conceptualization, M.S.; methodology, M.S. and H.X.; software, M.S. and L.H.; validation, M.S. and H.X.; formal analysis, M.S., Y.P. and C.Z.; investigation, M.S. and H.X.; resources, M.S.; data curation, M.S. L.H. and J.M.; writing—original draft preparation, M.S.; writing—review and editing, M.S.; visualization, M.S., Y.P. and C.Z.; supervision, M.S. and H.X.; project administration, M.S.; funding acquisition, M.S. All authors have read and agreed to the published version of the manuscript.

Funding: This study was supported by the National Key Research and Development Program of China (2020YFA0607502), the Basic Public Welfare Research Program of Zhejiang Province (LGF22D050004), and the Meteorological Bureau of Zhejiang Province (2021QN12).

Institutional Review Board Statement: Not applicable.

Informed Consent Statement: Not applicable.

Data Availability Statement: The datasets are available from the corresponding author on reasonable request.

Conflicts of Interest: The authors declare no conflict of interest.

References

1. World Meteorological Organization (WMO). WMO Greenhouse Gas Bulletin (GHG Bulletin) No. 17: The State of Greenhouse Gases in the Atmosphere Based on Global Observations through 2020. Available online: https://library.wmo.int/index.php?lvl=notice_display&id=21975#.Ysfo_TdBxD8 (accessed on 25 October 2021).
2. Bousquet, P.; Ciais, P.; Miller, J.B.; Dlugokencky, E.J.; Hauglustaine, D.A.; Prigent, C.; Van der Werf, G.R.; Peylin, P.; Brunke, E.G.; Carouge, C.; et al. Contribution of anthropogenic and natural sources to atmospheric methane variability. *Nature* **2006**, *443*, 439–443. [CrossRef] [PubMed]
3. Vaghjiani, G.L.; Ravishankara, A.R. New Measurement of the Rate Coefficient for the Reaction of OH with Methane. *Nature* **1991**, *350*, 406–409. [CrossRef]
4. Lelieveld, J.; Crutzen, P.J.; Dentener, F.J. Changing concentration, lifetime and climate forcing of atmospheric methane. *Tellus B* **1998**, *50*, 128. [CrossRef]
5. Shindell, D.; Kuylenstierna, J.C.I.; Vignati, E.; van Dingenen, R.; Amann, M.; Klimont, Z.; Anenberg, S.C.; Muller, N.; Janssens-Maenhout, G.; Raes, F.; et al. Simultaneously Mitigating Near-Term Climate Change and Improving Human Health and Food Security. *Science* **2012**, *335*, 183–189. [CrossRef] [PubMed]
6. Pu, J.J.; Xu, H.H.; Gu, J.Q.; Ma, Q.L.; Fang, S.X.; Zhou, L.X. Impacts of meteorological factors on atmospheric methane mole fractions in the background area of Yangtze River Delta. *Environ. Sci.* **2013**, *34*, 835–841.
7. Pu, J.J.; Xu, H.H.; Gu, J.Q.; Yu, X.M. Variation Characteristics of Atmospheric CH_4 Concentration at Lin'an Regional Background Station. *Resour. Environ. Yangtze Basin* **2012**, *21*, 79–83.
8. Yang, Q.; Guan, L.; Tao, F.; Liang, M.; Sun, W.Q. Changes of CH_4 Concentrations Obtained by Ground-based Observations at Five Atmospheric Background Stations in China. *Environ. Sci. Technol.* **2018**, *41*, 1–7. [CrossRef]
9. Xu, Y.; Liao, B.; Jiang, Z.; Xin, K.; Xiong, Y.; Guan, W. Emission of Greenhouse Gases (CH_4 And CO_2) Into The Atmosphere From Restored Mangrove Soil In South China. *J. Coastal. Res.* **2021**, *37*, 52–58. [CrossRef]
10. Tong, C.; Bastviken, D.; Tang, K.W.; Yang, P.; Yang, H.; Zhang, Y.; Guo, Q.; Lai, D.Y. Annual Co2 and Ch4 Fluxes in Coastal Earthen Ponds with Litopenaeus Vannamei in Southeastern China. *Aquaculture* **2021**, *545*, 737229. [CrossRef]

11. Liu, S.; Fang, S.; Liu, P.; Liang, M.; Guo, M.; Feng, Z. Measurement Report: Changing Characteristics of Atmospheric CH_4 In The Tibetan Plateau: Records From 1994 To 2019 At The Mount Waliguan Station. *Atmos. Chem. Phys.* **2021**, *21*, 393–413. [CrossRef]
12. Liang, M.; Zhang, Y.; Ma, Q.; Yu, D.; Chen, X.; Cohen, J.B. Dramatic decline of observed atmospheric CO_2 and CH_4 during the COVID-19 lockdown over the Yangtze River Delta of China. *J. Environ. Sci.* **2023**, *124*, 712–722. [CrossRef]
13. Liu, L.X.; Zhou, L.X.; Wen, M.; Zhang, F.; Fang, S.X.; Yao, B. Characteristics of Atmospheric CH_4 Concentration Variations at Four National Baseline Observatories in China. *Adv. Clim. Chang. Res.* **2009**, *5*, 41–46.
14. Fang, S.X.; Zhou, L.X.; Xu, L.; Yao, B.; Liu, L.X.; Xia, L.J.; Wang, H.Y. CH_4 Concentrations and the Variation Characteristics at the four WMO/GAW Background Stations in China. *Environ. Sci.* **2012**, *33*, 3–9.
15. Zhang, F.; Zhou, L.; Xu, L. Temporal variation of atmospheric CH4 and the potential source regions at Waliguan, China. *Sci. China Earth Sci.* **2013**, *56*, 727–736. [CrossRef]
16. Cheng, Y.; Shan, Y.; Xue, Y.; Zhu, Y.; Wang, X.; Xue, L.; Liu, Y.; Qiao, F.; Zhang, M. Variation characteristics of atmospheric methane and carbon dioxide in summertime at a coastal site in the South China Sea. *Front. Environ. Sci. Eng.* **2022**, *16*, 139. [CrossRef]
17. Pestunov, D.A.; Domysheva, V.M.; Sakirko, M.V.; Shamrin, A.M.; Panchenko, M.V. Methane in the atmosphere and surface water of Lake Baikal. In Proceedings of the 27th International Symposium on Atmospheric and Ocean Optics, Atmospheric Physics, Moscow, Russia, 5–9 July 2021; pp. 932–937.
18. Thoning, K.W.; Tans, P.P.; Komhyr, W.D. Atmospheric Carbon Dioxide at Mauna Loa Observatory 2. Analysis of the NOAA GMCC Data, 1974–1985. *J. Geophys. Res. Atmos.* **1989**, *94*, 8549–8565. [CrossRef]
19. Ruckstuhl, A.F.; Henne, S.; Reimann, S.; Steinbacher, M.; Vollmer, M.K.; O'Doherty, S.; Buchmann, B.; Hueglin, C. Robust extraction of baseline signal of atmospheric trace species using local regression. *Atmos. Meas. Tech* **2012**, *5*, 2613–2624. [CrossRef]
20. Gong, S.; Shi, Y. Evaluation of comprehensive monthly-gridded methane emissions from natural and anthropogenic sources in China. *Sci. Total Environ.* **2021**, *784*, 2613–2624. [CrossRef]
21. Li, P.; Yu, Y.; Zhao, S.P.; Dong, L.X.; Yan, M. Situation and Influencing Factors of Ground-level Ozone Pollution in China from 2015 to 2017. *Plateau Meteorol.* **2019**, *38*, 1344–1353. [CrossRef]
22. Wang, Y.Q.; Zhang, X.Y.; Draxler, R.R. TrajStat: GIS-based software that uses various trajectory statistical analysis methods to identify potential sources from long-term air pollution measurement data. *Environ. Model. Softw.* **2009**, *24*, 938–939. [CrossRef]
23. Yang, D.; Shen, S.; Zhang, M.; Lee, X.; Xiao, W. Uncertainty analysis on the estimation of CO_2 and CH_4 emission inventory over Nanjing and Yangtze River Delta. *J. Meteorol. Sci.* **2014**, *34*, 325–334. [CrossRef]